Commun Nonlinear Sci Numer Simulat 34 (2016) 12–22

Contents lists available at ScienceDirect

Commun Nonlinear Sci Numer Simulat

journal homepage: www.elsevier.com/locate/cnsns

Effects of the spike timing-dependent plasticity on the synchronisation in a random Hodgkin–Huxley neuronal network

R.R. Borges [a,b], F.S. Borges [a], E.L. Lameu [a], A.M. Batista [a,c,d,*], K.C. Iarosz [d], I.L. Caldas [d], R.L. Viana [e], M.A.F. Sanjuán [f]

[a] Pós-Graduação em Ciências, Universidade Estadual de Ponta Grossa, 84030-900 Ponta Grossa, PR, Brazil
[b] Departamento de Matemática, Universidade Tecnológica Federal do Paraná, 86812-460Apucarana, PR, Brazil
[c] Departamento de Matemática e Estatística, Universidade Estadual de Ponta Grossa, 84030-900Ponta Grossa, PR, Brazil
[d] Instituto de Física, Universidade de São Paulo, 05315-970 São Paulo, SP, Brazil
[e] Departamento de Física, Universidade Federal do Paraná, 81531-990Curitiba, PR, Brazil
[f] Departamento de Física, Universidad Rey Juan Carlos, Tulipán s/n,28933 Móstoles, Madrid, Spain

ARTICLE INFO

Article history:
Received 20 February 2015
Revised 2 October 2015
Accepted 7 October 2015
Available online 22 October 2015

Keywords:
Plasticity
Neuronal network
Synchronisation

ABSTRACT

In this paper, we study the effects of spike timing-dependent plasticity on synchronisation in a network of Hodgkin–Huxley neurons. Neuron plasticity is a flexible property of a neuron and its network to change temporarily or permanently their biochemical, physiological, and morphological characteristics, in order to adapt to the environment. Regarding the plasticity, we consider Hebbian rules, specifically for spike timing-dependent plasticity (STDP), and with regard to network, we consider that the connections are randomly distributed. We analyse the synchronisation and desynchronisation according to an input level and probability of connections. Moreover, we verify that the transition for synchronisation depends on the neuronal network architecture, and the external perturbation level.

1. Introduction

The human brain contains about 10^{11} neurons [1], and each neuron is connected to approximately 10^4 other neurons [2]. These connections called synapses, are arranged in a highly complex network. They are responsible for neuronal communication and can be classified into two categories: electrical and chemical synapses [3,4]. In electrical synapses the transmission of information from one neuron to another is directly performed from the pre-synaptic cell to the post-synaptic cell via gap junctions. In chemical synapses, the process occurs via neurotransmitters, which cross the synaptic cleft and bind to receptors on the membrane of the synaptic cell [5]. Neurotransmitters may increase or decrease the probability of an action potential of a post-synaptic neuron, and the synapses are called excitatory or inhibitory, respectively [6]. Furthermore, the intensity of the chemical synapses can be modified, in other words, they can be minimised or potentiated [7]. The mechanism responsible for these adjustments is known as synaptic plasticity [8].

* Corresponding author at: Departamento de Matematica e Estatistica, Universidade Estadual de Ponta Grossa, 84030-900 Ponta Grossa, PR, Brazil. Tel.: +55 4291446272.
E-mail address: antoniomarcosbatista@gmail.com (A.M. Batista).

http://dx.doi.org/10.1016/j.cnsns.2015.10.005
1007-5704/

The synaptic plasticity, that is, the ability of synapses to weaken or strengthen over time [9] is an important property of the mammalian brain. In addition, the synaptic plasticity is also related to processes of learning and memory [10,11]. This adjustment of the intensities of the chemical synapses can be correlated with phenomena of synchronisation of the neuronal firing [12].

Studies about synchronous behaviour has been shown to be of relevant importance in neuronal systems [13,14]. The occurrence of synchronisation in some specific areas of the brain may be associated with some diseases, such as the epilepsy and the Parkinson's disease [15–17]. On the other hand, it is also responsible for some vital brain functions, such as processing of sensory information and motor function [18,19].

Methods to suppress synchronisation have been proposed in neuroscience, as the introduction of external perturbations [20–23]. Tass and collaborators have verified the possibility of desynchronisation in hippocampal neuronal populations through coordinated reset stimulation [25]. Meanwhile, Popovych and collaborators have found that the introduction of a perturbation in a globally connected neuronal network combined with synaptic plasticity can provide a positive contribution to the firing synchronisation [22].

In this work, we study firing synchronisation in a random Hodgkin–Huxley neuronal network with plasticity according to spike timing-dependent plasticity (STDP). This synaptic plasticity model adjusts the connection strengths by means of the temporal interval between pre-synaptic and post-synaptic spikes [26,27]. Bi and Poo have reported that the change in synaptic efficiency after several repetitions of the experiment is due to the time difference of firing [28,29]. If one pre-synaptic spike precedes a post-synaptic spike, a long-term potentiation occurs, otherwise, a long-term depression appears [30].

A computational neuronal network specifies the connection architecture among neurons. A globally coupled Hodgkin–Huxley neuron model was also considered by Popovych and collaborators [22]. They studied the synchronisation behaviour considering STDP, and found that the mean synaptic coupling presents a dependence on the input level. In this work, we consider a random neuronal network with STDP, and input, where the connections are associated with chemical synapses [24]. One main result is to show that spike synchronisation in a neuronal network, depending on the probability of connections, can be improved due to spike timing-dependent plasticity. This improvement is also observed when an external perturbation is applied on the network. Another important result is that the orientation of the connections among neurons with a different spike frequency affect the synchronised behaviour.

This paper is organised as follows: in Section 2 we introduce the Hodgkin–Huxley neuronal model. In Section 3, we show the random neuronal network. In Section 4, we study the synchronisation considering spike timing-dependent plasticity. Finally, in the last Section, we draw the conclusions.

2. Hodgkin–Huxley neuronal network

2.1. Hodgkin–Huxley neuronal model

One of the most important models in computational neuroscience is the neuronal model proposed by Hodgkin and Huxley [31,32]. In this model, the mechanism of generation of an action potential was elucidated in a series of experiments with the squid giant axon. They found three different ions currents consisting of sodium (Na), potassium (K) and leak (L) mainly due to chlorine. Moreover, there are voltage-dependent channels for sodium, potassium that control the entry and exit of these ions through the cell. The model is composed of a system of four coupled differential equations given by

$$C\dot{V} = I - g_{\mathrm{K}} n^4 (V - E_{\mathrm{K}}) - g_{\mathrm{Na}} m^3 h (V - E_{\mathrm{Na}}) - g_{\mathrm{L}} (V - E_{\mathrm{L}}), \tag{1}$$

$$\dot{n} = \alpha_n(V)(1 - n) - \beta_n(V) n, \tag{2}$$

$$\dot{m} = \alpha_m(V)(1 - m) - \beta_m(V) m, \tag{3}$$

$$\dot{h} = \alpha_h(V)(1 - h) - \beta_h(V) h, \tag{4}$$

where C is the membrane capacitance (measured in μF/cm^2), V is the membrane potential (measured in mV), the function $m(V)$ and $n(V)$ are the variable of activation for sodium and potassium, and $h(V)$ is the variable of inactivation for sodium. The functions $\alpha_n, \beta_n, \alpha_m, \beta_m, \alpha_h, \beta_n$ are given by

$$\alpha_n(V) = \frac{0.01V + 0.55}{1 - \exp(-0.1V - 5.5)}, \tag{5}$$

$$\beta_n(V) = 0.125 \exp\left(\frac{-V - 65}{80}\right), \tag{6}$$

$$\alpha_m(V) = \frac{0.1V + 4}{1 - \exp(-0.1V - 4)}, \tag{7}$$

$$\beta_m(V) = 4 \exp\left(\frac{-V - 65}{18}\right), \tag{8}$$

$$\alpha_h(V) = 0.07 \exp\left(\frac{-V - 65}{20}\right), \tag{9}$$

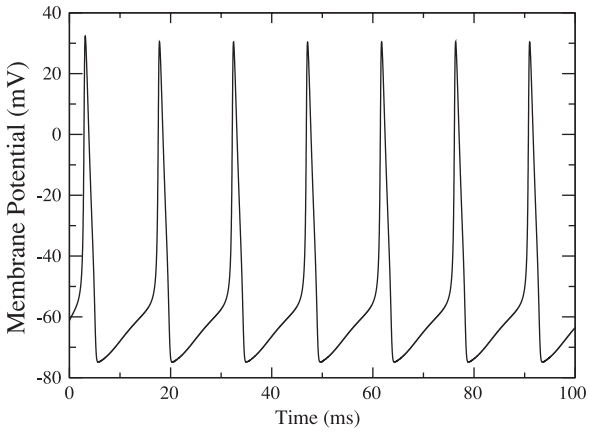

Fig. 1. Dynamic firing in the Hodgkin–Huxley model, where we consider $I = 10\,\mu$A/cm^2 that presents a regime with periodic firing.

Table 1
Parameters of the Hodgkin–Huxley neuronal model with a resting potential equal to −65 mV.

Description	Parameter	Values
Membrane capacity	C	1 μF/cm^2
Reversal potential for Na	E_{Na}	50 mV
Reversal potential for K	E_K	−77 mV
Reversal potential for L	E_L	−54.4 mV
Sodium conductance	g_{Na}	120 mS/cm^2
Potassium conductance	g_K	36 mS/cm^2
Leak conductance	g_L	0.3 mS/cm^2
External current	I	9.0 10.0 μA/cm^2

$$\beta_h(V) = \frac{1}{1+\exp(-0.1V-3.5)}. \tag{10}$$

The parameters g and E represent the conductance and reversal potentials for each ion, respectively, and the constant I is an external current density (measured in $\mu A/cm^2$). The Hodgkin–Huxley model was examined by Luccioli and collaborators [34] in its three fundamental dynamical regimes: silence, bistability, and repetitive firing. For small values ($I < 6.27\,\mu$A/cm^2) the Hodgkin–Huxley model is in a silent regime, namely the action potential is not initiated. In the interval 6.27 μ A/cm^2 $\leq I \leq$ 9.78 μ A/cm^2 the model presents bistability between silence and repetitive firing. The repetitive firing regime occurs for $I >$ 9.78 μ A/cm^2, as illustrated in Fig. 1 for $I = 10\,\mu$ A/cm^2. In our simulations, we consider the range 9 μ A/cm^2 $\leq I \leq$ 10 μ A/cm^2. For instance, $I = 9.0\,\mu$ A/cm^2 and $I = 10.0\,\mu$ A/cm^2 approximately correspond to 67 Hz and 70 Hz, respectively. Nevertheless, due to the fact that we are considering coupled neurons, there are always time intervals in that the total current applied to each neuron presents values larger than 9.78 μA/cm^2. In our simulations, we use the fourth-order Runge–Kutta method with a fixed step size equal to 10^{-2} ms, and we consider the parameters that are presented in Table 1 [33].

2.2. Network structure

Computational models of neuronal networks depend on the architecture, which specifies how neurons are connected and how the dynamics is applied to each unit or node. In this work, we consider a random network, that is, the network is constructed by connecting neurons randomly [35–37]. Each connection is included with probability independent from every other connection. Fig. 2 exhibits a schematic representation of the neuronal network considered in this work. Each neuron is connected to others by randomly chosen neurons with probability p. When $p = 1$ we have a global network, where all neurons are connected.

We consider a random neuronal network with chemical synapses where the connections are unidirectional, and the local dynamics is described by the Hodgkin–Huxley model. The network is given by

$$C\dot{V}_i = I_i - g_K n^4(V_i - E_K) - g_{Na} m^3 h(V_i - E_{Na}) - g_L(V_i - E_L) + \frac{(V_r - V_i)}{\omega}\sum_{j=1}^{N}\varepsilon_{ij}s_j + \Gamma_i, \tag{11}$$

where V_i is the membrane potential of neuron i ($i = 1, \ldots, N$), I_i is a constant current density randomly distributed in the interval [9.0, 10.0], ω is the average degree connectivity, and ε_{ij} is the coupling strength from the pre-synaptic neuron j to the post-synaptic neuron i. The values of ε_{ij} are normally distributed with mean and standard deviation equal to 0.1 and 0.02, respectively,

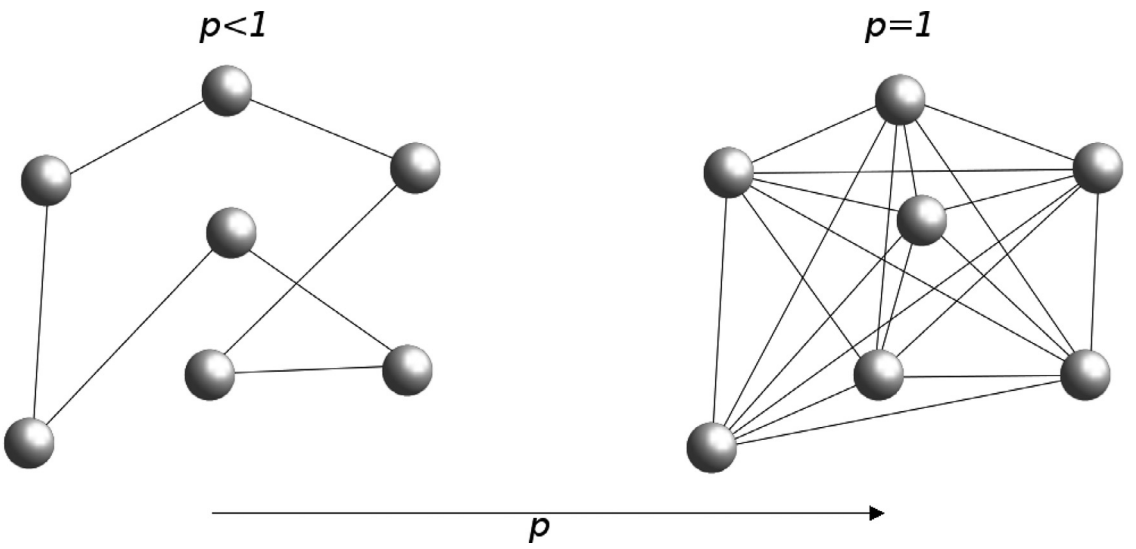

Fig. 2. Schematic representation of a network in which each neuron is connected to others by randomly chosen neurons with probability p.

when connections exist, otherwise $\varepsilon_{ij} = 0$ for lacking connections [30]. The lower and upper bounds of the synaptic weights are equal to 0.0 and 0.5, respectively. We consider an external perturbation Γ_i in that the value of γ is equal for all the neurons. In each time step ρ equal to 10^{-2}ms a random input with amplitude γ is applied to each neuron with a probability equal to $\rho/14$. The value of 14 ms is approximately the inter-spike interval of a single neuron. In other words, throughout the simulation at each time step one number is generated for each neuron from a random generator that returns a uniform random deviate between 0 and 1, and if this number is smaller than $\rho/14$, the neuron is perturbed. As a result, in the interval of 14 ms all the neurons are perturbed. The neurons are excitatory coupled with a reversal potential $V_r = 20$ mV [22]. The post-synaptic potential s_i is given by [38,39]

$$\frac{ds_i}{dt} = \frac{5(1 - s_i)}{1 + \exp\left(-\frac{V_i+3}{8}\right)} - s_i. \tag{12}$$

2.3. Spiking neurons synchronisation

When identical neurons are coupled, the network may exhibit a complete synchronisation among spiking neurons, i.e., all neurons have identical time evolution of their action potential. We do not consider identical neurons here, and due to this fact, a complete synchronisation is not possible. However, a weak synchronisation may be observed.

As diagnostic of spikes synchronisation we use the order parameter given by [40,41]

$$R = \left| \frac{1}{N} \sum_{j=1}^{N} \exp\left(i\psi_j\right) \right|, \tag{13}$$

where

$$\psi_j(t) = 2\pi m + 2\pi \frac{t - t_{j,m}}{t_{j,m+1} - t_{j,m}}, \tag{14}$$

where $t_{j,m}$ denotes when a spike m ($m = 0, 1, 2, \dots$) of a neuron j occurs ($t_{j,m} < t < t_{j,m+1}$). The beginning of each spike is considered when $V_j > 0$. If the spikes times are uncorrelated, their contribution to the result of the summation is small [42]. However, in a globally synchronised state the order parameter magnitude asymptotes the unity.

Fig. 3 (a and b) present raster plots of spike onsets where the latter are indicated by dots. For $p = 0.1$ and without external perturbation, shown in Fig. 3(a), the neuronal network presents asynchronous dynamics. Considering $p = 1.0$, we have globally coupled neurons, and we can see that the network exhibits synchronised spiking, shown in Fig. 3(b). The time evolution of the order parameter is plotted in Fig. 3(c). When $p = 0.1$ (black line), the network does not display synchronised behaviour, and as a result the order parameter is typically small with R fluctuating around 0.1. However, synchronised behaviour is observed for $p = 1.0$ with order parameter values near unity (red line).

We add an external perturbation (Γ_i) to analyse its effects on the synchronous behaviour. This way we compute the time averaged magnitude of the order parameter, given by

$$\bar{R} = \frac{1}{t_{\text{fin}} - t_{\text{ini}}} \sum_{t=t_{\text{ini}}}^{t_{\text{fin}}} R(t), \tag{15}$$

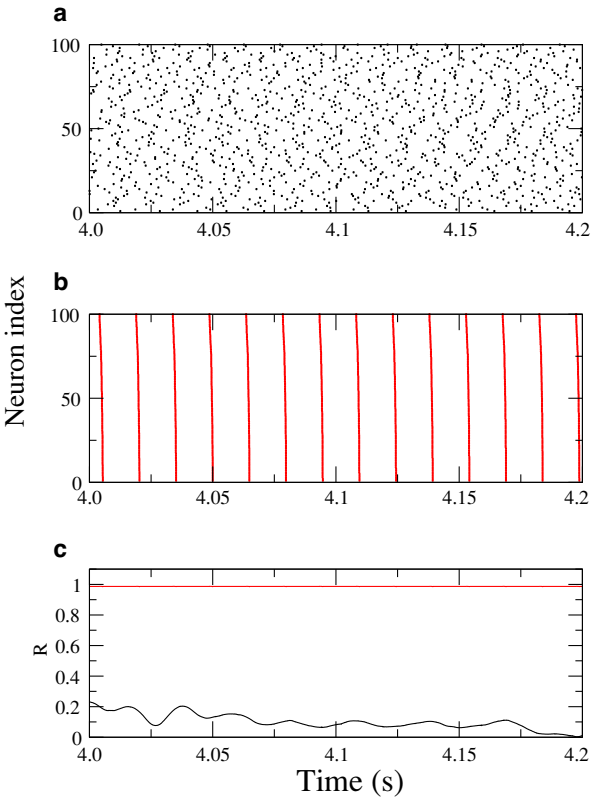

Fig. 3. Raster plots of spike onsets where the latter are indicated by dots for $N = 100$, (a) $p = 0.1$, and (b) $p = 1.0$. In (c) the order parameter is calculated for $p = 0.1$ (black line), and $p = 1.0$ (red line). The constant current density I_i is randomly distributed in the interval [9.0, 10.0], and for different initial conditions we have obtained the same dynamical behaviour. (For interpretation of the references to colour in this figure legend, the reader is referred to the web version of this article.)

where the values of $\bar{R}$ have been computed by averaging over a temporal length of 10 s after discarding a transient of 490 s ($t_{\text{ini}} = 490$ s and $t_{\text{fin}} = 500$ s). In Fig. 4 we can see the time averaged order parameter as a function of the probability for different input amplitudes (γ). When the neuronal network has no input, it is possible to observe synchronised behaviour if the probability of connection is large enough (black circles). However, external inputs are able to desynchronise the spiking neurons, as shown in Fig. 4 for $\gamma = 5$ (red triangles) and $\gamma = 10$ (blue squares), where the values of $\bar{R}$ are less than 0.9.

3. Spike timing-dependent plasticity

One of the key principles of behavioural neuroscience is that experience can modify the brain structure, that is known as neuroplasticity [43]. Although the idea that experience may modify the brain structure can probably be traced back to the 1890 s [44,45], it was Hebb who made this a central feature in his neuropsychological theory [46].

With this in mind, we consider spike timing-dependent plasticity according to the Hebbian rule. In this plasticity the coupling strength ε_{ij} is adjusted based on the relative timing between the spikes of pre-synaptic and post-synaptic neurons [28],

$$\Delta\varepsilon_{ij} = \begin{cases} A_1 \exp\left(-\Delta t_{ij}/\tau_1\right), & \Delta t_{ij} \geq 0 \\ -A_2 \exp\left(\Delta t_{ij}/\tau_2\right), & \Delta t_{ij} < 0 \end{cases}, \tag{16}$$

where $\Delta t_{ij} = t_i - t_j = t_{\text{pos}} - t_{\text{pre}}$. Fig. 5 exhibits the result that is obtained from Eq. (16) for $A_1 = 1.0$, $A_2 = 0.5$, $\tau_1 = 1.8$ ms, and $\tau_2 = 6.0$ ms. The plasticity function (16) was obtained by Bi and Poo [47] from experimental results, where long-term depression ($\Delta t_{ij} < 0$) and long-term potentiation ($\Delta t_{ij} \geq 0$) windows were each fitted with an exponential function.

The initial synaptic weights ε_{ij} are normally distributed with mean and standard deviation equal to 0.1 and 0.02, respectively. Then, they are updated according to Eq. (16), where $\varepsilon_{ij} \to \varepsilon_{ij} + 10^{-3}\Delta\varepsilon_{ij}$. In our simulations, we consider that the STDP update rule is not applied to connections that are initially lacking, namely we do not consider the creation of synapses. In addition, if neurons are disconnected, they will continue disconnected. In the absence of an external perturbation, we can verify by means of Fig. 6(a) that the averaged synaptic weights can be depressed ($p = 0.3$) or potentiated ($p = 0.5$, $p = 0.7$, and $p = 1.0$) depending on the probability of connections. The averaged synaptic weight is given by $\bar{\varepsilon}_{ij} = (1/M)\sum_{i,j\in\Theta}\varepsilon_{ij}$, where the synapse is from neuron i to neuron j with both of them in a set Θ of synapses randomly distributed, and M is the total number of synaptic

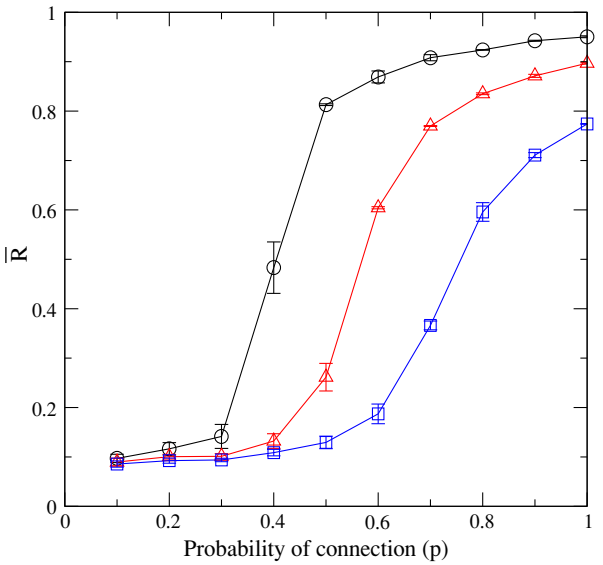

Fig. 4. Average order parameter as a function of the probability, for $N = 100$, for I_i randomly distributed in the interval [9.0, 10.0], for external perturbation with $\gamma = 0$ (black circles), $\gamma = 5$ (red triangles), and $\gamma = 10$ (blue squares). The bars represent the standard deviation for different initial conditions. (For interpretation of the references to colour in this figure legend, the reader is referred to the web version of this article.)

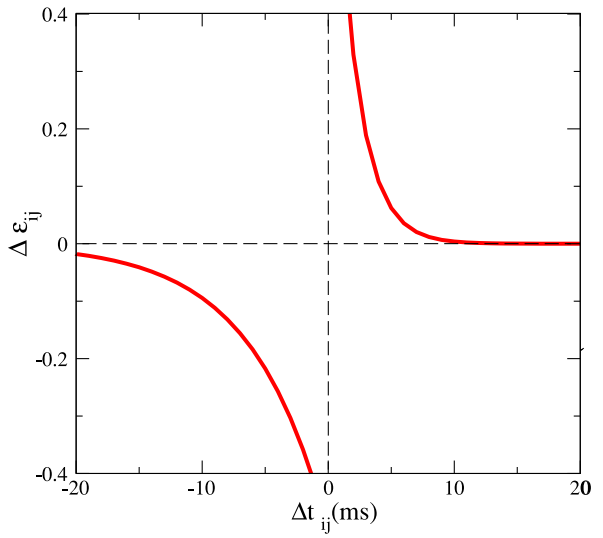

Fig. 5. Plasticity function (16) as a function of the difference of spike timing of post- and pre-synaptic neuron.

weights. If an input is applied on the neuronal network (Fig. 6(b)), the input can have a constructive effect on the synaptic weights ($p = 0.7$ and $p = 1.0$) or destructive effect ($p = 0.3$ and $p = 0.5$), depending on the probability of connections.

The time averaged order parameter in terms of the probability of connection is showed in Fig. 7, considering with (black circles) and without (red triangles) STDP. Each point represents the mean of $\bar{R}$ taken from different initial condition profiles, where we consider 15 different initial conditions for the coupling strength and for the connections. In the case for without external perturbation (Fig. 7(a)) we can see that the values of $\bar{R}$ without STDP are less than with STDP, namely STDP is producing a positive effect on the synchronisation. A stronger coupling may lead to a stronger synchronisation for the unperturbed network. For a large value of the probability of connections a stronger coupling leads to a stronger synchronisation. However, if the probability of connections is not large, a stronger coupling may not lead to a stronger synchronisation. In this case, the synchronisation also depends on the network architecture. Pade and Pereira [48] showed that improving the structure of a directed network can lead to instabilities in the synchronised behaviour. In our results, we verify for the unperturbed network that the enhancing effect of the STDP on the spike synchronisation, illustrated in Fig. 7(a), is approximately 14% for $p = 0.5$, 9% for $p = 0.6$, and 3% for

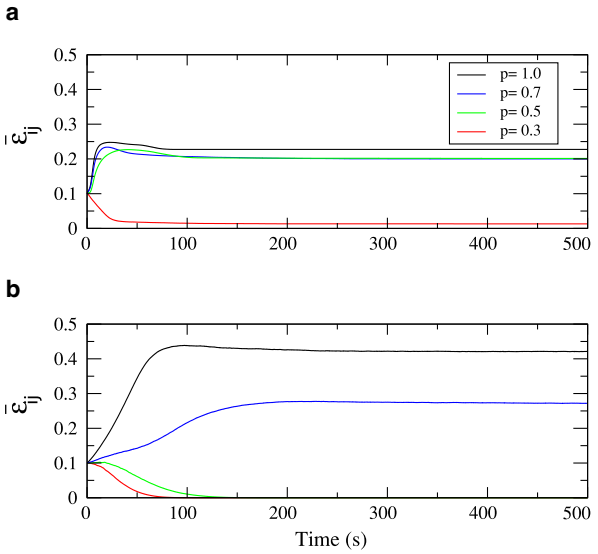

Fig. 6. Time evolution of the averaged coupling strength for $p = 0.3$ (red line), $p = 0.5$ (green line), $p = 0.7$ (blue line), and $p = 1.0$ (black line), where it is considered (a) $\gamma = 0$, and (b) $\gamma = 5$. The direction of the synapse is from the neuron i to the neuron j. The constant current density I_i is randomly distributed in the interval [9.0, 10.0], and for different initial conditions we have obtained the same dynamical behaviour. (For interpretation of the references to colour in this figure legend, the reader is referred to the web version of this article.)

$p = 1$. Increasing the amplitude of the external perturbation, without spike timing-dependent plasticity, the desynchronisation is induced in the neuronal network (Fig. 4). However, considering STDP in the perturbed network is possible to observe alterations to the dynamic behaviour in relation to synchronised states. Fig. 7(b) shows that the STDP enhances the synchronisation for p approximately greater than 0.5 due to a constructive effect on the dynamics of the synaptic weights. On the other hand, for p less than 0.5 the STDP decreases the values of the time averaged order parameter, as a result of depressed synaptic weights. Increasing the input intensity ($\gamma = 5$), it is possible to verify synchronisation when the network has neuroplasticity (Fig. 7(c)). We can also see an abrupt transition from a desynchronised to a synchronised regime. When the input intensity increases, it is necessary to increase the probability of connection for the STDP counteracts the suppression of synchronisation. Fig. 7(d) exhibits a situation such that the synchronisation is only obtained when the neuronal network presents a global coupling ($p = 1$). With a strong input, the STDP does not lead the network to a potentiation of synaptic weights, and this way the synchronisation is suppressed by an external input.

The spike synchronisation depends on the probability of connections p in a way showing an abrupt transition. There is a critical point for $p = p_c$ that can be found by means of the intersection between the curves of potentiation and depression. Fig. 8(a) exhibits the point of intersection with value of Δt_{ij} approximately equal to 1.8. For $\Delta t_{ij} > 1.8$ the depression (red line) of the synaptic strength is larger than the potentiation (black line), while that for $\Delta t_{ij} < 1.8$ the potentiation is larger than the depression. When phase-locked neurons fire with the time lag greater than 1.8 ms, the STDP depresses the coupling strength and the neurons eventually desynchronise. With this value of Δt_{ij} we can obtain p_c plotting $\Delta\bar{t}_{ij}$ as a function of p, as shown in Fig. 8(b). It can be seen that the value of $\Delta\bar{t}_{ij}$ decays, and when cross the value $\Delta\bar{t}_{ij} \approx 1.8$ we have the critical value of the probability of connections. Moreover, when p increases not only $\Delta\bar{t}_{ij}$ decreases, but also the standard deviation of the inter-spike intervals decreases. Then, we compute the critical probability as a function of the input level (Fig. 8(c)), where we verify a linear increase given by the equation $p_c = 0.06\gamma + 0.37$. The critical connection probability remains unchanged for other initial conditions for coupling due to the fact that the average time difference (Fig. 8(b)) is calculated from different initial condition profiles.

Fig. 7 (c) shows a discontinuous transition between the synchronised and the desynchronised regime. Our aim is to understand how this discontinuous transition appears when the probability of connections is varied. For this reason, we build a network according to a schematic representation that is showed in Fig. 9. The scheme represents a network of neurons with high (cyan ball) and low (yellow ball) spiking frequency. The red arrows represent the connections between neurons from high to low frequency, while the black arrows represent the connections from low to high frequency.

Based on the schematic representation that is illustrated in Fig. 9, we consider a neuronal network with $N = 100$, $p = 0.47$, and $\gamma = 3$. We separate the neuronal network into 50 neurons with high frequency (values of I_i within the range [9.0,9.1]) and 50 neurons with low frequency (values of I_i within the range [9.9,10]). Fig. 10 exhibits the time averaged coupling strength as a function of the percentage of connections from neurons with high frequency to neurons with low frequency. We can see that the time average coupling strength depends on the connections. Considering the case for a small percentage of connections from

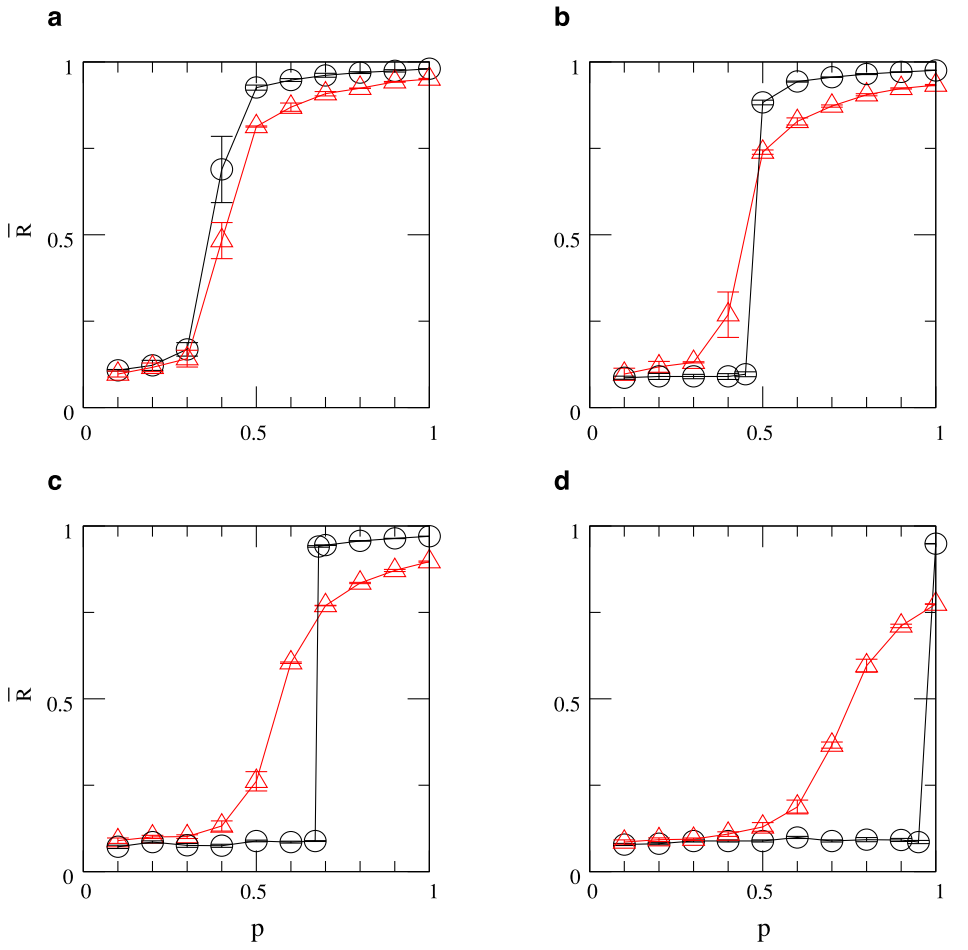

Fig. 7. Average order parameter versus probability of connection for the cases with (black circles) and without (red triangles) STDP, where we consider (a) $\gamma = 0$, (b) $\gamma = 3$, (c) $\gamma = 5$, and (d) $\gamma = 10$. The constant current density I_i is randomly distributed in the interval [9.0, 10.0], and the bars represent the standard deviation for different initial conditions. (For interpretation of the references to colour in this figure legend, the reader is referred to the web version of this article.)

HFN to LFN, the average coupling is small, indicating absence of synchronisation, a situation that changes with increasing the percentage of connections to a synchronised state. This means that, when the coupling strengths increase, a desynchronised state can suddenly become synchronised. Consequently, the abrupt transition from desynchronised to synchronised state, that is observed in Fig. 7, is due to directed synapses among spiking neurons with high and low frequency. Bayati and Valizadeh [49], as well as Popovich and collaborators [22], showed that directed synapses from the high frequency neurons to the low frequency neurons tend to be potentiated while the synapses from the low frequency neurons are weakened. They verified this behaviour in an all-to-all network equipped with the STDP. In our simulations, we consider a random network with STDP and the novelty is that due to directed synapses the neuronal network can present an abrupt transition to the spike synchronisation when the probability of connections increases.

4. Conclusion

We have been studying a neuronal network model with spiking neurons. We have chosen, as local dynamics, the Hodgkin–Huxley model due to the fact that it has essential features of spiking dynamics. The Hodgkin–Huxley model is a coupled set of nonlinear differential equations that describes the ionic basis of the action potential. These equations are able to reproduce biophysical properties of the action potential.

We have used a random coupling architecture where the connections are randomly distributed according to a probability. When the probability is equal to unity we have a globally coupled network. The connections were considered unidirectional representing excitatory chemical synapses.

We have studied the effects of spike timing-dependent plasticity on the synchronisation in a Hodgkin–Huxley neuronal network. Studies about spike synchronisation are important to understand not only progressively degenerative neurological

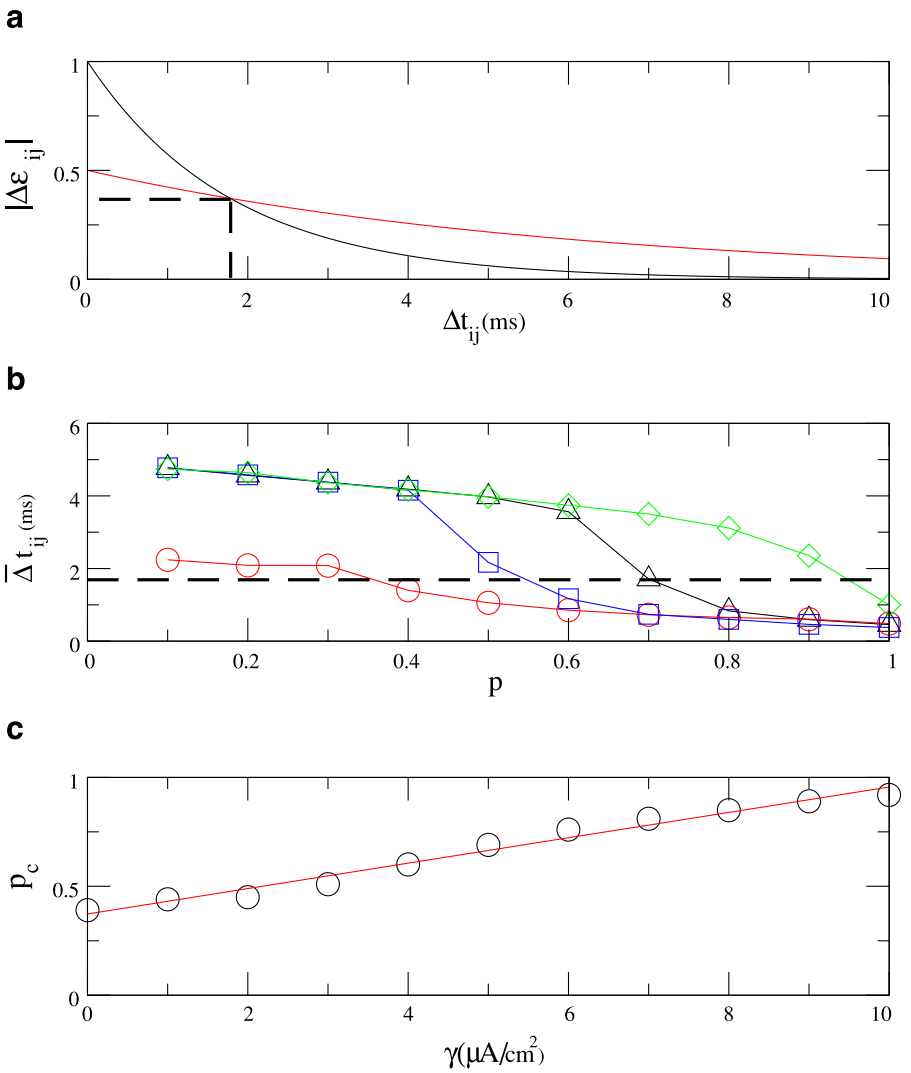

Fig. 8. (a) Absolute value of the plasticity function (16) as a function of the difference of spike timing of post- and pre-synaptic neuron, where the curves are the potentiation (black line) and the depression (red line). (b) Average time difference versus probability of connections for $\gamma = 0$ (red circles), $\gamma = 3$ (blue squares), $\gamma = 5$ (black triangles), and $\gamma = 10$ (green diamonds). (c) Critical probability p_c as a function of the input level γ. The linear fit is given by the equation $p_c = 0.06\gamma + 0.37$. (For interpretation of the references to colour in this figure legend, the reader is referred to the web version of this article.)

disorders, but also processing of the sensory information. Popovych and collaborators [22] showed that STDP combined with an external perturbation can improve the spike synchronisation in a globally neuronal network. The novelty in this paper is that we have considered a random neuronal network and we have verified that the spike synchronisation depend on the probability of connections. Considering a strong external perturbation the spike synchronisation is suppressed. However, when there is STDP, depending on the probability of connections, the synchronisation in the perturbed network can be improved due to a constructive effect on the synaptic weights.

We have also shown that the direction of synapses has an important role on the effects of spike timing-dependent plasticity on the synchronisation in a random Hodgkin–Huxley neuronal network. In addition, we have not observed any relationship between the probability of connection and the percentage of connections from HFN to LFN. Certainly, this is due to the topology of the neuronal network with random connectivity that we have considered in this work. We believe that other topologies may present a relationship between the connectivity and this percentage.

We have carried out simulations considering a coupling strength normally distributed, and different initial profiles for the connectivity. As a result, we have not verified any dependence on the initial conditions for the coupling, except for the value of p where the transition from desynchronised to synchronised behaviour is abrupt (Fig. 7(c)). In this abrupt transition, we verify a form of multistability due to the directed synapses. Therefore, in future works, we plan to study with more detail the existence of multistability in the neuronal network model studied in this work.

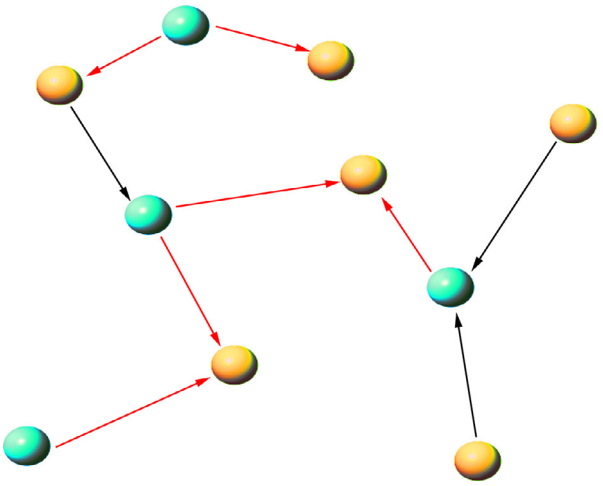

Fig. 9. Schematic representation of a network of neurons with high (cyan ball) and low (yellow ball) spiking frequency. The red arrows represent the connections between neurons from high to low frequency, while the black arrows represent the connections from low to high frequency. (For interpretation of the references to colour in this figure legend, the reader is referred to the web version of this article.)

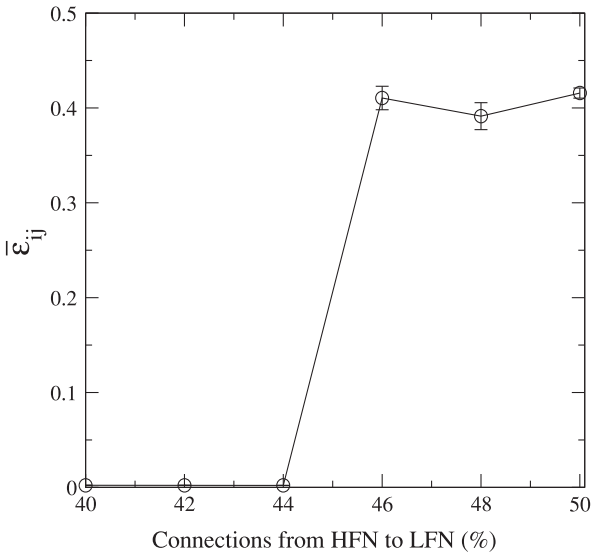

Fig. 10. Time averaged coupling strength versus percentage of connections from neurons with high frequency (HFN) to neurons with low frequency (LFN). We consider $p = 0.47$ and $\gamma = 3$. The direction of the synapse is from the neuron i to the neuron j.

Acknowledgements

This study was possible by partial financial support from the following Brazilian government agencies: CNPq, CAPES and FAPESP (2011/19296-1 and 2015/07311-7). Financial support by the Spanish Ministry of Economy and Competitivity under project number FIS2013-40653-P is also acknowledged.

References

[1] Chialvo DR. Critical brain networks. Phys A 2004;340:756–65.
[2] Gerstner W, Kistler W. Spiking neuron models: Single neurons, populations, plasticity. 1st. Cambridge: Cambridge University Press; 2002.
[3] Bear MF, Connors BW, Paradiso MA. Neuroscience: exploring the brain. 3rd. England: Lippincott Williams and Wilkins; 2006.
[4] Byrne JH. Fundamental neuroscience. San Diego: Academic Press; 2008.
[5] Dayan P, Abbott LF. Theoretical neuroscience: computational and mathematical modelling of neural systems. 1st. Massachusetts: Mit Press; 2001.
[6] Purves D, Augustine DJ, Fitzpatrick D, Hall WC, LaMantia A-S, McNamara JO, et al. Neuroscience. 3rd. Massachusetts: Sinauer Associates Inc Publishers; 2004.
[7] Dagostin AA, Mello CV, Leão RM. Increased bursting glutamatergic neurotransmission in an auditory forebrain area of the zebra finch (Taenopygia guttata) induced by auditory stimulation. J Comp Physiol A 2012;198:705–16.
[8] Hebb D. The organization of behavior. New York: Wiley; 1949.

[9] Citri A, Malenka RC. Synaptic plasticity: multiple forms, functions, and mechanisms. Neuropsychopharmacol 2008;33:18–41.
[10] Kelso SR, Ganong AH, Brown TH. Hebbian synapses in hippocampus. Proc Natl Acad Sci USA 1986;83:5326–30.
[11] Caporale N, Dan Y. Spike timing-dependent plasticity: a Hebbian learning rule. Annu Rev Neurosci 2008;31:25–46.
[12] Zhigulin VP, Rabinovich MI, Huerta R, Abarbanel HD. Robustness and enhancement of neural synchronization by activity-dependent coupling. Phys Rev E 2003;67:021901.
[13] Arenas A, Díaz-Guilera A, Kurths J, Moreno Y, Zhou C. Synchronisation in complex networks. Phys Rep 2008;469:93–153.
[14] Timme M, Wolf F, Geisel T. Topological speed limits to network synchronization. Phys Rev Lett 2004;92:074101.
[15] Abuhassan K, Coyle D, Maguire L. Compensating for thalamocortical synaptic loss in Alzheimers disease. Front Comput Neurosci 2014;8:65.
[16] Modolo J, Bhattacharya B, Edwards R, Campagnaud J, Legros A, Beuter A. Using a virtual cortical module implementing a neural field model to modulate brain rhythms in Parkinsons disease. Front Neurosci 2010;4:45.
[17] Hammond C, Bergman H, Brown P. Pathological synchronization in Parkinsons disease: networks, models and treatments. Trends Neurosci 2007;30:357–64.
[18] Nini A, Feingold A, Slovin H, Bergman H. Neurons in the globus pallidus do not show correlated activity in the normal monkey, but phase-locked oscillations appear in the MPTP model of parkinsonism. J Neurophysiol 1995;74:1800–5.
[19] Uhlhass P, Singer W. Neural synchrony in brain disorders: relevance for cognitive dysfunctions and pathophysiology. Neuron 2006;52:155–68.
[20] Lameu EL, Batista CAS, Batista AM, Iarosz KC, Viana RL, Lopes SR, et al. Suppression of bursting synchronization in clustered scale-free (rich-club) neuronal networks. Chaos 2012;22:043149.
[21] Popovych OV, Tass PA. Desyncrhonizing electrical and sensory coordinated reset neuromodulation. Front Hum Neurosci 2012;6:58.
[22] Popovych OV, Yanchuk S, Tass PA. Self-organized noise resistance of oscillatory neural networks with spike timing-dependent plasticity. Sci Rep 2013;3:2926.
[23] Luccioli S, Ben-Jacob E, Barzilai A, Bonifazi P, Torcini A. Clique of functional hubs orchestrates population bursts in developmentally regulated neural networks. Plos Comput Biol 2014;10:e1003823.
[24] Nordenfelt A, Used J, Sanjuán MAF. Bursting frequency versus phase synchronization in time-delayed neuron networks. Phys Rev E 2013;87:052903.
[25] Tass PA, Silchenko AN, Hauptmann C, Barnikol UB, Speckmann E-J. Long-lasting desynchronization in rat hippocampal slice induced by coordinated reset stimulation. Phys Rev E 2009;80:011902.
[26] Feldman DE. The spike-timing dependence of plasticity. Neuron 2012;75:556–71.
[27] Markram H, Gerstner W, Sjöström PJ. Spike-timing-dependent plasticity: a comprehensive overview. Front Synaptic Neurosci 2012;4:8.
[28] Bi GQ, Poo MM. Synaptic modifications in cultured hippocampal neurons: dependence on spike timing, synaptic strength, and postsynaptic dell type. J Neurosci 1998;18:10464–72.
[29] Gerstner W, Sprekeler H, Deco G. Theory and simulation in neuroscience. Sci 2012;338:60–5.
[30] Gray EG. Electron microscopy of synaptic contacts on dendrite spines of the cerebral cortex. Nature 1959;183:1592–3.
[31] Hodgkin AL, Huxley AF. A quantitative description of membrane current and its application to conduction and excitation in nerve. J Physiol 1952;117:500–44.
[32] Izhikevich EM. Which model to use for cortical spiking neurons? IEEE Trans Neur Netw 2004;15:1063–70.
[33] Izhikevich EM. Dynamical systems in neuroscience: the geometry of excitability and bursting. 1st. London: MIT Press; 2006.
[34] Luccioli S, Kreuz T, Torcini A. Dynamical response of the Hodgkin–Huxley model in the high-input regime. Phys Rev E 2006;73:041902.
[35] Erdös P, Rényi A. On random graphs I. Publ Math 1959;6:290–7.
[36] Nordenfelt A, Wagemakers A, Sanjuán MAF. Frequency dispersion in the time-delayed Kuramoto model. Phys Rev E 2014a;89:032905.
[37] Nordenfelt A, Wagemakers A, Sanjuán MAF. Cyclic motifs as the governing topological factor in time-delayed oscillator networks. Phys Rev E 2014b;90:052920.
[38] Destexhe A, Mainen ZF, Sejnowki TJ. An efficient method for computing synaptic conductances based on a kinetic model of receptor binding. Neural Comput 1994;6:14–18.
[39] Golomb D, Rinzel J. Dynamics of globally coupled inhibitory neurons with heterogeneity. Phys Rev E 1993;48:4810.
[40] Kuramoto Y. Self-entralnment of a population of coupled non-linear oscillators. Int Symp Math Probl Theor Phys 1975;39:420–3.
[41] Kuramoto Y. Chemical oscillations, waves, and turbulence. Dover, editor. Berlin: Springer Berlin Heidelberg; 1984.
[42] Acebrón JA, Bonilla LL, Vicente CJP, Ritort F, Spigler R. The Kuramoto model: a simple paradigm for synchronization phenomena. Rev Mod Phys 2005;77:137–85.
[43] Ramón y Cajal S, May MM. Degeneration & regeneration of the nervous system. London: Oxford University Press; 1928.
[44] Bliss TVP, Gardner-Medwin AR. Long-lasting potentiation of synaptic transmission in the dentate area of the unanaestherised rabbit following stimulation of the perforant path. J Physiol 1973;232:357–74.
[45] Bliss TVP, Collingridge GL. A synaptic model of memory: long-term potentiation in the hippocampus. Nature 1993;361:31–9.
[46] Hebb DO. Brain mechanisms and learning. London: Oxford University Press; 1961.
[47] Bi GQ, Poo MM. Synaptic modification by correlated activity: Hebb's postulated revisited. Annu Rev Neurosci 2001;24:139–66.
[48] Pade JP, Pereira T. Improving network structure can lead to functional failures. Sci Rep 2015;9968:1–6.
[49] Bayati M, Valizadeh. Effect of synaptic plasticity on the structure and dynamics of disordered networks of coupled neurons. Phys Rev E 2012;86:011925.